

TENSION STIFFENING OF REINFORCED HIGH-STRENGTH CONCRETE TENSION MEMBERS

S.V.T. Janaka PERERA^{*1}, Hiroshi MUTSUYOSHI^{*2}, Nay Myo NYUNT^{*3} and Hikaru WATANABE^{*4}

ABSTRACT

Direct tension tests were performed on reinforced high-strength concrete (RHSC) members. Using the results obtained from the experiments, the effect on tension stiffening was examined. The test results showed not only were splitting cracks along the reinforcement more extensive, but also the transverse crack spacing became smaller. Thereby, the reduction in the tension stiffening effect in high-strength concrete (HSC) is much greater than that would be expected. Based on the present results, a new empirical model is proposed to predict tension stiffening of HSC members.

Keywords: cracking, high-strength concrete, tension members, tension stiffening

1. INTRODUCTION

The recent trend of employing reinforced high-strength concrete (RHSC) with a concrete strength of over 100 MPa has resulted in smaller member sizes which leads to higher tension stress in the reinforcement. Therefore, it is becoming increasingly necessary to understand the deformation compatibility conditions when designing RHSC structures. In order to do this, the tension stiffness of concrete, which plays an important role in the deformation behavior of the reinforced concrete (RC) structures in the post-cracking region of concrete, needs to be considered.

Although concrete is assumed to carry no tension at crack locations, it is still able to develop tensile stresses between the cracks through the transfer of bond forces from the reinforcement to the concrete. Tension stiffening arises from this ability of concrete to carry tension between cracks in an RC member, and helps control member stiffness, deformation, and crack widths related to satisfying serviceability requirements [1]. Fig. 1 shows overall tension stiffening behavior as outlined by the CEB-FIP model code [2].

According to past studies, the relationship between concrete strength and tension stiffness of concrete has not been clarified [1-5]. In fact, in numerical methods such as the modified compression field theory (MCFT), tension stiffness is not dependent on concrete strength [3]. However, a previous numerical study found that the tension stiffness of high-strength concrete (HSC) is lower than that of normal-strength concrete (NSC) [6]. Other variables such as the percentage and distribution of reinforcing steel, bar size, bond properties, and shrinkage of concrete are also reported to have an effect on tension stiffening [1]. Fig. 2 shows the wide range of results

predicted by various empirical models developed for tension stiffening in RC, all of which demonstrate a reduction in tensile capacity of cracked concrete with increasing strain. It seems tension stiffness of HSC cannot be accurately predicted by current models.

Therefore, the objective of this paper is to experimentally evaluate the tension stiffness of axially loaded tension members of HSC and to propose a new more accurate model to predict tension stiffness of HSC members.

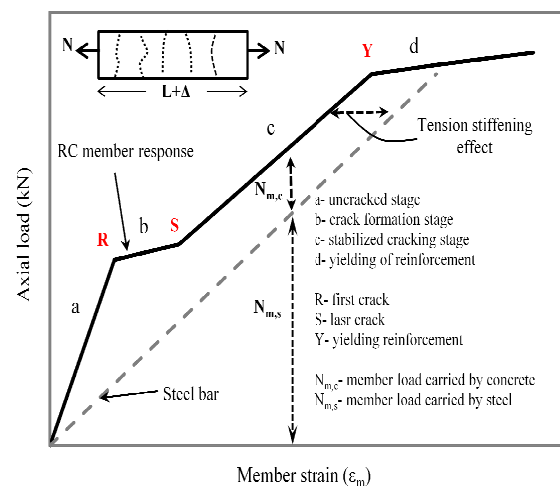


Fig. 1 Idealized behavior of RC ties.

2. TENSION STIFFENING PREDICTION

A number of empirical relationships have been proposed for tension stiffening, where the loss of rigidity in a cracked member can be taken into account for the stress-strain response of the steel or an average

*1 Graduate Student, Graduate School of Science and Engineering, Saitama University, JCI Member
 *2 Professor, Graduate School of Science and Engineering, Saitama University, JCI Member
 *3 Graduate Student, Graduate School of Science and Engineering, Saitama University
 *4 Graduate Student, Graduate School of Science and Engineering, Saitama University

stress-strain response for concrete in the post-cracking range. Eq. (1) (Fig. 2) uses a combination of both [7]. Collins and Mitchell [8] considered a load-sharing concept to account for tension stiffening, where axial load N is carried by both the steel and concrete (Eq. (2), Fig. 2).

For any given axial member strain ϵ_m , the average load carried by the concrete $N_{m,c}$ is obtained by subtracting the respective average steel force from the member response as shown in Fig. 1. The average stress in the concrete f_c is then determined using effective concrete area A_c , giving $f_c = N_{m,c}/A_c$. The average concrete stress can then be normalized with the concrete cracking strength f_{cr} . The normalized stress β ($= f_c/f_{cr}$) accounts for the variation of tensile stresses in the concrete between cracks. Belarbi and Hsu [7] propose using $\beta = (\epsilon_{cr}/\epsilon_m)^{0.4}$, while Collins and Mitchell [8] suggest a value of $\beta = (1 + \sqrt{500\epsilon_m})^{-1}$.

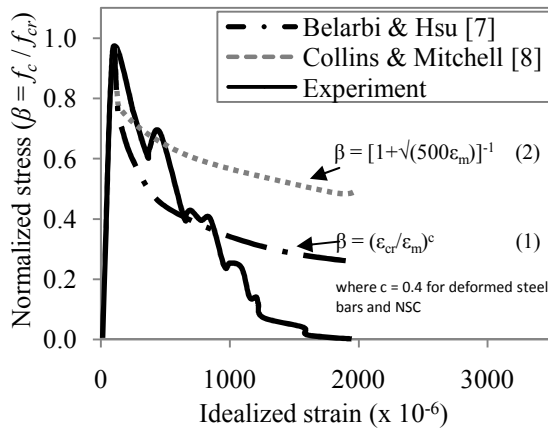


Fig. 2 Empirical models reported for tension stiffening factor β .

3. TEST PROGRAMS

3.1 Details of Materials and Specimens

Testing was carried out on ten specimens that were axially loaded. Fig. 3 shows the geometry and instrumentation for a typical test specimen. All of the specimens had a length of 1200 mm. A single deformed steel bar, with a minimum concrete cover of 40 mm, was provided. Tension stiffening was evaluated for NSC (40 to 60 MPa) and HSC (100 to 150 MPa) using reinforcement ratios (ρ) of 1.99 and 2.252% respectively. The yield strength and Young's modulus of steel were 722 MPa and 202.5 GPa respectively. The

concrete mix proportions are tabulated in Table 1. The concrete properties are shown in Table 2. The diameters of reinforcement bars were selected to prevent the effect of splitting cracks since they are not significant when concrete cover to bar diameter (c/d_b) is larger than 2.5 [5]. Details of specimens are given in Table 2.

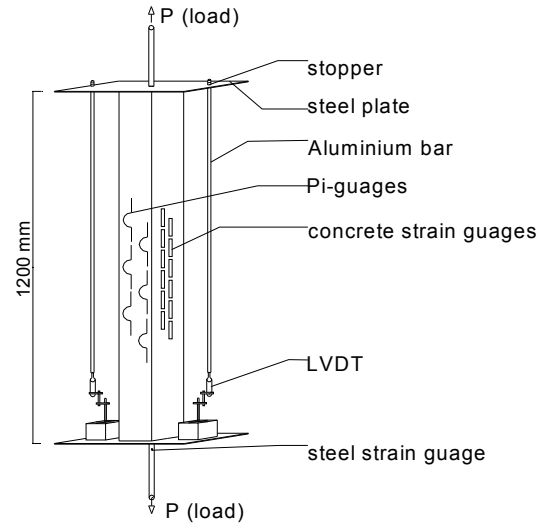


Fig. 3 Test setup

3.2 Loading Method

Specimens were loaded vertically through one-axial tension rods. Two linear variable displacement transducers (LVDT) were clamped to the steel reinforcing bar just outside of the concrete to measure the total elongation of the reinforced concrete specimen (Fig. 3). At each load stage, the cracks were measured using pi-gauges. The complete response of each specimen was described by plotting the applied tension against the average member strain.

Average early-age shrinkage was determined for all concretes from strain measurements on 100x100x400 mm shrinkage specimens that had the same moisture curing conditions as the tension specimen. Shrinkage was included in analysis of the member response by using the calculated shrinkage strain value from the early-age shrinkage specimens to determine the initial strain for each tension specimen (Table 2). The initial strain was taken as an offset strain equal to $\epsilon_{sh}/[1 + n\rho]$; where ϵ_{sh} is concrete early-age shrinkage, n is modular ratio (E_s/E_c), ρ is reinforcing steel ratio, E_s is Young's modulus of steel, and E_c is

Table 1 Mix proportions of concrete

Name of concrete	W/B (%)	Unit weight (kg/m ³)						
		W	OPC	SF	S	G	SP	DA
NSC30	58	178	307	-	825	1040	-	-
NSC50	46	168	363	-	757	1017	3.45	-
HA80	30	160	-	534	873	795	6.94	0.53
HA120	20	155	-	775	703	792	11.63	0.78
HA160	17	155	-	912	592	792	14.59	0.91

B= OPC + SF

B: Binder, W: Water

OPC: Ordinary Portland cement

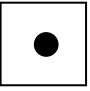
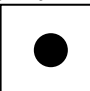
SF: Silica fume cement, S: Sand

G: Gravel (maximum size of aggregate is 20mm)

SP: Super plasticizer

DA: Air reducing admixture

Table 2 Specimen properties and test results

Specimen	d_b (mm), c/d_b	Cross-section dimensions (mm)	Concrete strength		Strain		Initial cracking load		L (mm)
			f'_c (MPa)	f_t (MPa)	ε_{sh} ($\times 10^{-6}$)	ε' ($\times 10^{-6}$)	T (kN)	S (kN)	
NSC30-D16	16, 2.6	100x100, cover 40mm 	40	3.21	-101	-89	21.9	95.0	133
NSC50-D16			56	3.88	-126	-111	28.5	70.0	133
HA80-D16			102	5.73	-223	-201	27.6	52.0	82
HA120-D16			125	7.13	-244	-223	40.6	58.0	80
HA160-D16			145	6.89	-317	-289	33.2	52.0	71
NSC30-D25	25, 2.5	150x150, cover 40mm 	40	3.21	-101	-88	60.5	156	145
NSC50-D25			56	3.88	-126	-109	55.4	135.5	153
HA80-D25			102	5.73	-223	-198	73.0	117.5	128
HA120-D25			125	7.13	-244	-220	111.5	123.0	126
HA160-D25			145	6.89	-317	-286	70.1	109.0	116

d_b : Steel bar diameter, c : Concrete cover, f'_c : Compressive strength of concrete

f_t : Splitting tensile strength of concrete, ε_{sh} : Early-age shrinkage, ε' : Offset strain ($\mu\varepsilon = \varepsilon_{sh}/[1 + n\rho]$)

T: Transverse crack, S: Splitting crack, L: Average transverse crack spacing

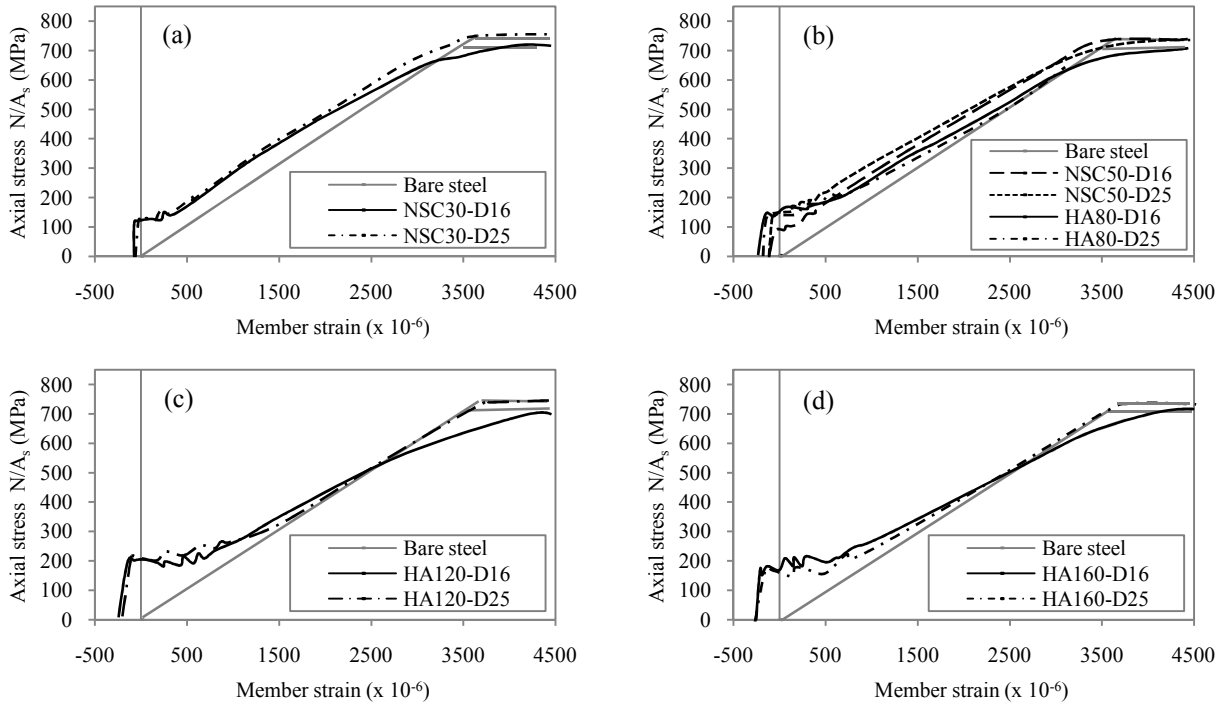


Fig. 4 Tension versus average strain response of normal-strength and high-strength concrete specimens

elastic modulus of concrete [1]. Shrinkage strains were assumed to be uniform over the cross section. Subtracting shrinkage strains from the member response gives an idealized concrete member strain, equivalent to a member with no shrinkage.

4. RESULTS AND DISCUSSION

4.1 Cracking Behavior

The average tensile strength of NSC and HSC was used to gain a better understanding of cracking behavior. According to tension members' test results, the average tensile strengths of NSC and HSC (> 100 MPa) were $0.37f'_c{}^{0.5}$ and $0.32f'_c{}^{0.5}$ (MPa) respectively. Also, the corresponding elastic modulus of E_c for NSC and HSC was equal to $4030f'_c{}^{0.5}$ and $3270f'_c{}^{0.5}$ (MPa)

respectively. This results in an estimated cracking strain of $92 \mu\varepsilon$ for NSC and $98 \mu\varepsilon$ for HSC. However, observed cracking strains were $90 \mu\varepsilon$ on average for NSC and $100 \mu\varepsilon$ for HSC.

Fig. 4 shows a comparison of the measured load-deformation response including shrinkage strains. The HSC specimens exhibited a larger cracking load than NSC specimens. As the concrete strength increased roughly four-fold, from 40 MPa to 145 MPa, the transverse cracking load increased by approximately 1.3 times (Table 2). However, the splitting cracking loads decreased by approximately 40%. According to the experimental results, the relative transverse cracking load in the specimens matched the increase in the splitting-tensile strength of concrete. Therefore, transverse cracks were directly affected by

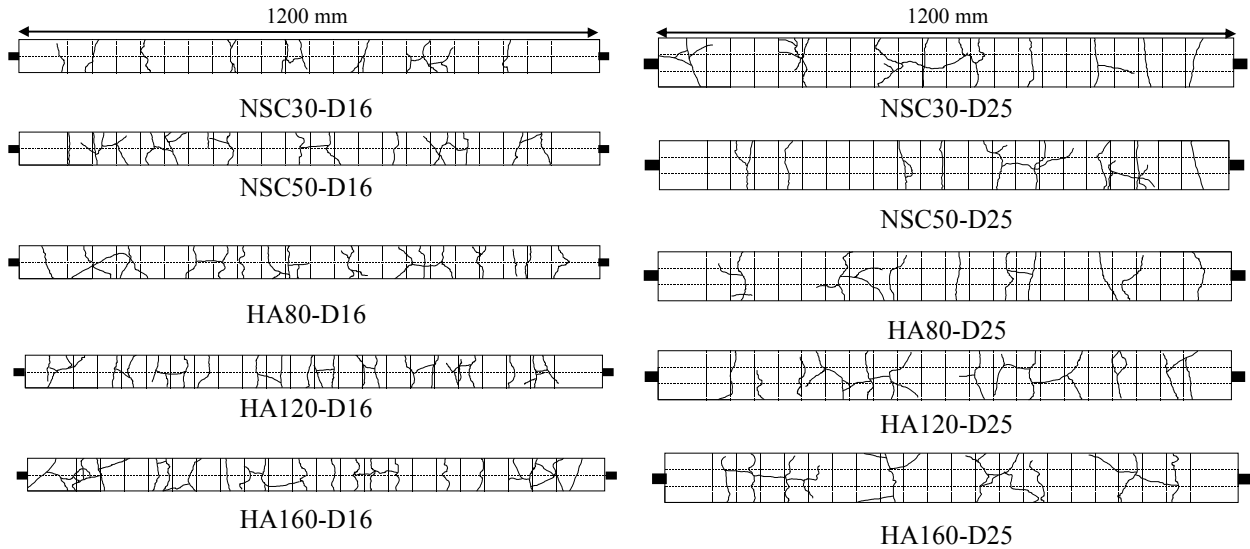
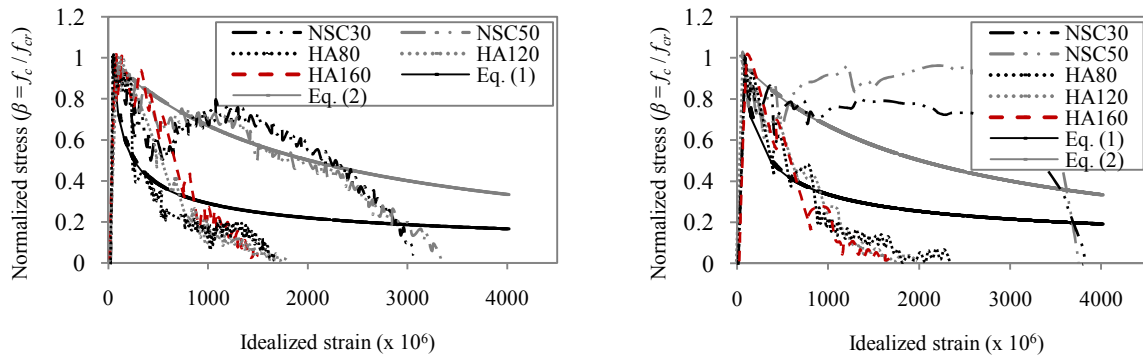


Fig.5 Final crack configuration in NSC and HSC specimens



(a) D16 specimens

(b) D25 specimens

Fig. 6 Normalized tensile material behavior of concrete specimens

concrete tensile strength. However, splitting cracking strength was not affected by concrete splitting-tensile strength.

The transverse cracking load to splitting cracking load (T/S) ratio was increased when concrete strength increased from 40 to 125 MPa (Table 2). At concrete strength 125 MPa, the differences of the load between S and T were 17.4 and 11.5 kN in HA120-D16 and HA120-D25 respectively. However, at concrete strength 145 MPa, a decrease in the T/S ratio was seen.

One of the important facts observed in Fig. 5 is that the crack spacing significantly decreased with an increase in concrete strength. As the compressive strength of concrete increased from 40 MPa to 145 MPa, the average transverse crack spacing decreased by 10-50 % in both steel bar sizes (Table 2). This result contradicts that of Abrishami and Mitchell that found that crack spacing increases in HSC [5].

4.2 Influence of Concrete Strength on Tension Stiffening

Fig. 4 compares the influence of concrete strength on the responses of specimens reinforced with 16 and 25 mm bar sizes. This comparison clearly shows that the effect of tension stiffening at the stabilized cracking stage decreased with increasing concrete strength (Fig. 4 (b)). This result obviously contradicts

past studies. For example, Abrishami and Mitchell [5] showed that HSC specimens with a strength of 90 MPa exhibit a larger tension stiffening after cracking than the NSC specimens. This behavior is clearly attributed to the early splitting cracks and excessive progress along the rebar with the increase in load. At the concrete splitting cracks along the rebar, the bond between the bar and the concrete was diminished. Therefore, the concrete is no longer able to share the tensile force, in turn resulting in a large deformation with a small stiffening effect.

The tension stiffening reduction in HSC members can be further explained using elastic theory. According to elastic theory, the bond behavior of HSC can be quantitatively drawn. Since the elastic modulus of concrete is a function of compressive strength, while that of steel remains constant, the composite structural system consisted of reinforcement and concrete is altered with concrete strength, which results in a different stress state in the interface. Furthermore, HSC is more brittle than NSC [9], and in turn, less stress redistribution can take place at the ultimate loading stage. These two material properties in HSC change the crack spacing and tensile stiffness of tension members [10].

Fig. 6 shows a comparison of the measured normalized stress (β) response with the curves predicted

by Eq. (1) and (2). The predictions by Eq. (1) underestimates the normalized stresses of NSC members, while overestimate that of HSC ($f'_c > 100$ MPa) members. The model proposed by Collins and Mitchell [8] also overestimates the normalized stresses of HSC members. Also, it overestimates member stresses of NSC members during the early cracking and underestimates the member stresses once cracking has stabilized.

From the above results and discussion, it can be concluded that the effect of material characteristics of HSC is not accounted for by Eq. (1) and (2). Therefore, to predict tension stiffening reduction in Eq. (1) $\beta = (\varepsilon_{cr}/\varepsilon_m)^c$, a larger value for constant c need to be used. Also, a reduction coefficient to account for this influence is required in Eq. (2).

$$\beta = K[1 + \sqrt{500\varepsilon_m}]^{-1} \quad (3)$$

where K is tension stiffening reduction factor; $K=1.0$ for deformed steel bars and NSC [6].

5. Predictions of Tension Stiffening

5.1 Applicability of Existing Models for HSC

To check the applicability of existing models for both NSC and HSC members, Eq. (1) and (3) were compared with experimental results as shown in Fig. 7. A best fit curve for the test results was obtained by changing each constant c and K in both Eq. (1) and (3) respectively.

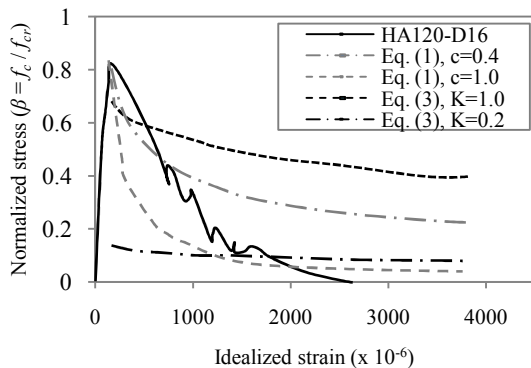
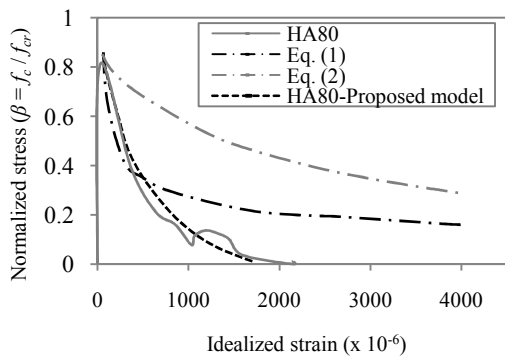


Fig. 7 Applicability of existing models for HSC ties



(a) Normalized stress

According to analysis results, Eq. (1) can predict tension stiffening of HSC members with larger c value. However, predictions underestimate the response of members (Fig. 7). For concrete strength over 100 MPa, the recommended c value is 0.9 (Table 3). The predictions of Eq. (2) with a smaller K value underestimate the member response during the early stages of crack development (Fig. 7). For HSC members, best fit K value is 0.2 (Table 3). From these two models, Eq. (1) was found to be more reliable for design purposes.

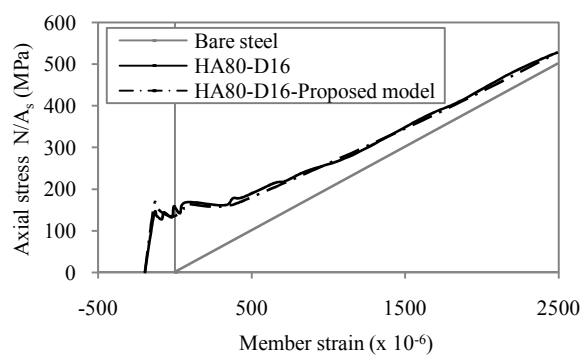
5.2 Proposed Model for HSC

As discussed previously, the present experimental results show that the tension stiffness of axially loaded members is highly dependent on concrete strength. According to Figures 2 and 7, tension stiffness of HSC members after cracking cannot be sufficiently predicted by available models. Therefore, a new model is proposed to predict normalized stress, β , of HSC tension members. A best fit to the test results is obtained by using the following prediction equation.

$$\beta = 2.5(1 - 0.135 \ln \varepsilon_m) \quad (4)$$

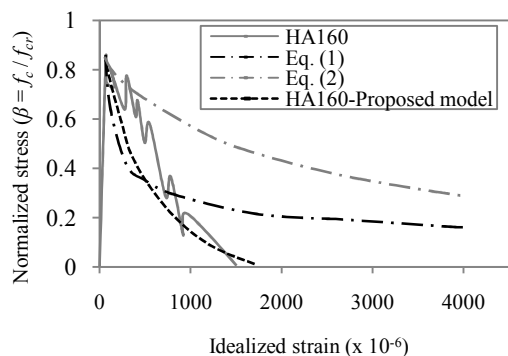
Table 3 Recommended constants for exiting models

Specimen	Constants obtained from experiment	
	Eq. (1), c	Eq. (3), K
NSC30-D16	0.3	1.0
NSC50- D16	0.2	1.0
HA80- D16	0.8	0.2
HA120- D16	1.0	0.2
HA160- D16	0.9	0.2
NSC30- D25	0.2	1.0
NSC50- D25	0.2	1.0
HA80- D25	0.8	0.2
HA120- D25	0.9	0.2
HA160- D25	1.0	0.2

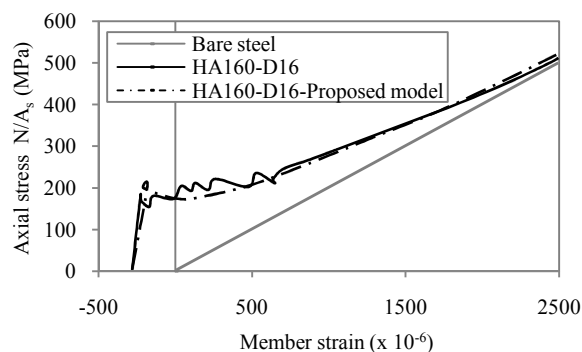


(b) Axial stress

Fig. 8 Comparison between test results and predicted response for HA80-D16



(a) Normalized stress



(b) Axial stress

Fig. 9 Comparison between test results and predicted response for HA160-D16

This model is valid for HSC tension members with a concrete strength over 100 MPa. Eq. (4) was examined by comparing with the experimental normalized stress and load-deformation curves as illustrated in Figures 8 and 9, and it can be seen that the new model provides more accurate predictions for HSC tension members.

6. CONCLUSIONS

Tension stiffening behavior of both NSC and HSC was investigated. Direct tension tests were performed on tension members with five concrete strengths (40, 50, 100, 125, 145 MPa) with two steel bar sizes (16, 25 mm) as major variables. The results of a test series of 10 tension specimens were presented and analyzed. Based on the results of this study, the following conclusions are drawn:

- (1) It is observed that the tension stiffening effect is highly dependent on concrete strength when it is greater than 100 MPa.
- (2) As the concrete strength increased from 40 MPa to 145 MPa, the tension stiffening effect became smaller for members with a c/d_b ratio of 2.5.
- (3) The crack spacing between the adjacent transverse cracks becomes narrower as higher concrete strength is used, and a reduction in crack spacing of 10-50% was observed when the compressive strength of concrete varied from 40 MPa to 145 MPa.
- (4) A more accurate tension stiffening prediction equation is suggested for the design of HSC members.
- (5) The present Belarbi & Hsu [7] and Collins & Mitchell [8] equations for evaluating the tension stiffening of HSC members need to be modified as suggested in this paper.

REFERENCES

- [1] Fields, K. and Bischoff, P.H., "Tension Stiffening and Cracking of High-Strength Reinforced Concrete Tension Members". *ACI Structural Journal*, Vol. 101, No. 4, July-August 2004, pp. 447-456.
- [2] CEB-FIP. "CEB-FIP Model Code 1990", Comite Euro-International Du Beton, Paris, France, 1991.
- [3] Bentz, E.C., "Sectional Analysis of Reinforced Concrete Members", PhD dissertation, Dept. Civil Engineering, University of Toronto, Toronto, 2000.
- [4] Maekawa, K., Pimanmas, A., and Okamura, H., "Nonlinear Mechanics of Reinforced Concrete", Spon Press, London, 2003, pp.565-651.
- [5] Abrishami, H.H. and Mitchell, D., "Influence of Splitting Cracks on Tension Stiffening", *ACI Structural Journal*, Vol. 93, No. 6, Nov.-Dec. 1996, pp. 703-710.
- [6] Perera, S.V.T.J., Mutsuyoshi, H. and Asamoto, S., "Properties of High-Strength Concrete", *Proc. of 12th International Summer Symposium of Japan Society of Civil Engineers (JSCE)*, Funabashi-Japan, 2010.
- [7] Belarbi, A., and Hsu, T.T.C., "Constitutive Laws of Concrete in Tension and Reinforcing Bars Stiffened by Concrete", *ACI Structural Journal*, Vol. 91, No. 4, July-Aug. 1994, pp. 465-474.
- [8] Collins, M.P., and Mitchell, D., "Prestressed Concrete Structures", Prentice-Hall, Inc., Englewood Cliffs, N.J., 1991, pp. 766.
- [9] Perera, S.V.T.J., Mutsuyoshi, H., Takeda, R. and Asamoto, S. "Shear Behavior of High Strength Concrete Beams", *Proc. of Japan Concrete Institute (JCI)*, 32-2, pp. 685-690, Saitama-Japan, 2010.
- [10] Lee, G.Y., and Kim, W., "Cracking and Tension Behavior of High-Strength Concrete Tension Members Subjected to Axial Load", *Advances in Structural Engineering*, A Multi-Science Publication, Vol. 12, 2009, pp. 127-137.